A Letters Journal Exploring the Frontiers of Physics

December 2008

EPL, **84** (2008) 64002
doi: 10.1209/0295-5075/84/64002

www.epljournal.org

Spontaneous channeling of solitary pulses in heated-film flows

B. Scheid[1(a)], S. Kalliadasis[2], C. Ruyer-Quil[3] and P. Colinet[1]

[1] *Laboratoir TIPs, Université Libre de Bruxelles - CP 165/67, 1050, Bruxelles, Belgium, EU*
[2] *Chemical Engineering, Imperial College London - SW7 2AZ, London, UK, EU*
[3] *Laboratoire FAST/UMR-CNRS 7608 - Campus Universitaire, 91405, Paris, France, EU*

received 17 September 2008; accepted in final form 14 November 2008
published online 12 January 2009

PACS 47.15.gm – Thin film flows
PACS 47.54.-r – Pattern selection; pattern formation
PACS 47.55.dm – Thermocapillary effects

Abstract – We investigate the dynamics of a liquid film flowing down a uniformly heated wall. We use a four-field weighted-average model for the film thickness, the surface temperature and the two-dimensional flow rate vector. Time-dependent simulations are rationalized in a phase diagram. For small Reynolds numbers we observe regularly spaced rivulets aligned with the flow that prevent the development of hydrodynamic waves while for large Reynolds numbers, the evolution is similar to that observed in the isothermal case, *i.e.* wave-dominated. The transition between the two regimes is characterized by an intricate-pattern formation dynamics, including regimes of quasi-2D solitary pulses riding the crests of rivulets.

An isothermal liquid film falling down a vertical plane is an intriguing hydrodynamic phenomenon that exhibits a sequence of wave instabilities and transitions which are generic to a large class of hydrodynamic and other nonlinear systems: after several spatial/temporal transitions of (naturally excited) unstable disturbances the initially 2D wave evolution gives way to a fully developed 3D wave regime. This stage of the evolution is "weak/dissipative turbulence": indeed despite the apparent complexity one can still identify 3D pulses in what appears to be a randomly disturbed surface (see, *e.g.*, [1]). 3D pulses then become elementary processes so that the dynamics of the system can be described as a superposition of these pulses [2]. Hence, a falling liquid film can serve as a canonical reference system for the study of weak/dissipative turbulence. Three-dimensional hydrodynamic waves have been investigated experimentally by various authors [3–5] who have provided a clear picture of the phenomenology and intricate dynamics of interacting 3D waves in isothermal film flows.

When the falling film is uniformly heated from the wall, as encountered in thin-film evaporators and cooling of electronics, its dynamics is influenced, in addition to inertia and surface tension, by the variation of surface tension with temperature, namely the long-wave thermocapillary (Marangoni) effect [6–8], which possibly leads to rivulet-like structures aligned with the flow as predicted by linear stability analysis [9]. Joo *et al.* [10] modeled the nonlinear stage of such rivulet structures by incorporating the Marangoni effect into the *Benney equation* (MBE). The Benney equation in the absence of the Marangoni effect (BE) is the simplest nonlinear film evolution equation that accounts for inertia and thus includes the basic physics of hydrodynamic waves in falling liquid films [11,12]. However, the validity of BE, and thus MBE, is restricted to small Reynolds numbers ($Re \lesssim 1$). Indeed both models experience a finite-time blow-up at some $Re = O(1)$, which was shown in both cases to be due to the high-order nonlinearities originating from inertia [13]. This blow-up is clearly unphysical as shown by comparison with direct numerical simulations (DNS) in the case of heated falling films [14]. In isothermal conditions, though a regularized version of BE [15] does predict instead saturated solitary waves in the inertia-dominated regime ($Re > 1$), it is known to unrealistically underpredict the amplitude and phase speed of waves [16].

In this letter we examine the 3D wave dynamics of a vertical heated falling film in the region where inertia (hydrodynamic) and thermocapillary instabilities are equally important, *i.e.* $Re \gtrsim 1$. We propose a model of four evolution equations for the film thickness h, the streamwise and transverse flow rates averaged across the film, q and p, respectively, and the interfacial temperature θ, all dependent only on time t and in-plane coordinates

(a) E-mail: bscheid@ulb.ac.be

(x,z), with x along the main flow and z in the transverse direction. Slow time and space modulations of the basic flat-film state have been assumed, namely $\partial_t,\ \partial_x,\ \partial_z \sim \varepsilon \ll 1$ where ε is an ordering parameter. Having posed self-similar profiles in terms of the natural similarity variable $\bar{y} = y/h$ (y being the cross-stream coordinate), namely a parabolic profile for the velocity $f_0(\bar{y}) = \bar{y} + (1/2)\bar{y}^2$ and a linear profile for the temperature $g_0(\bar{y}) = \bar{y}$, the model has been obtained by averaging along the thickness the momentum and energy equations with weights taken equal to f_0 and g_0, respectively, like in the Galerkin method (details of the procedure are given in [17] for the 2D case). Provided the no-slip condition applies on the wall and the viscous stresses balancing the (thermo)capillary effects at the free surface, the weighted average momentum equation at order ε has the form

$$\partial_t \mathbf{q} = \frac{5}{6} h\,\mathbf{i} - \frac{5}{2}\frac{\mathbf{q}}{h^2} - \frac{5}{4} Ma \boldsymbol{\nabla}\theta + \frac{5}{6}\Gamma h \boldsymbol{\nabla}(\boldsymbol{\nabla}^2 h) + \frac{9}{7}\left(\frac{\mathbf{q}\cdot\boldsymbol{\nabla}h}{h^2} - \frac{\mathbf{q}}{h}\cdot\boldsymbol{\nabla}\right)\mathbf{q} - \frac{8}{7}\frac{\boldsymbol{\nabla}\cdot\mathbf{q}}{h}\,\mathbf{q},$$

where $\boldsymbol{\nabla} = (\partial_x, \partial_z)$, $\mathbf{q} = (q,p)$ and $\mathbf{i}$ is the streamwise unit vector. The first four terms of the r.h.s. account for the gravity acceleration, viscous shear stress, Marangoni effect and surface tension, respectively, and the remaining terms are due to inertia. Then, provided the temperature field is uniform at the wall and satisfies Newton's law of cooling at the free surface, the weighted average energy equation at order ε has the form

$$\partial_t \theta = 3\frac{(1-\theta-Bih\theta)}{Pr\,h^2} + \frac{7}{40}(1-\theta)\frac{\boldsymbol{\nabla}\cdot\mathbf{q}}{h} - \frac{27}{20}\frac{\mathbf{q}\cdot\boldsymbol{\nabla}\theta}{h},$$

where the first term of the r.h.s accounts for the in-depth heat transfer and the remaining terms are due to heat convection. The system is closed by mass conservation

$$\partial_t h + \boldsymbol{\nabla}\cdot\mathbf{q} = 0.$$

The lengthscale and timescale are $l_\nu = (\nu^2/g)^{1/3}$ and $t_\nu = (\nu/g^2)^{1/3}$, with ν the kinematic viscosity and g the gravitational acceleration. The governing dimensionless groups are the Kapitza number $\Gamma = \sigma l_\nu/\rho\nu^2$, the Marangoni number $Ma = \gamma\Delta T l_\nu/\rho\nu^2$, the Biot number $Bi = \alpha l_\nu/k$ and the Prandtl number $Pr = \nu/\chi$, with ρ the density, σ the surface tension and $\gamma = -\mathrm{d}\sigma/\mathrm{d}T$ its variation with temperature, ΔT the temperature difference between the wall and the ambient gas, α the heat transfer coefficient at the liquid-gas interface, k the thermal conductivity and χ the thermal diffusivity. The Reynolds and Weber numbers appear implicitly through the thickness of the uniform flat film h_N as $Re = gh_\mathrm{N}^3/3\nu^2$ and $We = \sigma/\rho g h_\mathrm{N}^2$. All numbers are taken of $O(1)$, except $\Gamma \sim We = O(\varepsilon^{-2})$. For isothermal conditions ($Ma = 0$), the present model reduces to the $O(\varepsilon)$-version of the 3D model given in [18], validated against both DNS and experiments. Notice that the coefficients in the momentum and energy equations differ from unity because of the non-uniformity of the base state profiles, precisely represented by f_0 and g_0. For example $5/6 = (\int_0^1 f_0)^2/\int_0^1 f_0^2$ and $9/7 = \int_0^1 f_0^3/(\int_0^1 f_0^2 \int_0^1 f_0)$. These coefficients are necessary to recover the MBE obtained in [10] through a gradient expansion of the present model in the limit $Re \ll 1$.

For both numerical purposes and presentation of the results, the thickness is rather scaled by h_N and the time by $\nu We^{1/3}/gh_\mathrm{N}$ in what follows. A pseudo-spectral scheme has been employed to solve the above system of equations, details and validation of which will be reported in a separate study. The computational domain is periodic of size $2\pi/k_x \times 2\pi/k_z$, where $k_x = 2k_z = 0.05$. The initial condition is white noise of maximum amplitude $1/1000^{\mathrm{th}}$ of h_N. Computations are terminated when the film thickness reaches a "minimal thickness" of about $h \sim 10^{-3}$ for which long-range intermolecular forces cannot be neglected. Consequently, we refer to *rupture* when the film reaches this minimal thickness, independently of the subsequent dynamics that depends on the nature of these intermolecular forces (see, *e.g.*, [19]). Parameters are those corresponding to a water film at 20 °C ($\Gamma = 3375$, $Pr = 7$) with $\Delta T = 2.8$ °C ($Ma = 25$) and $\alpha = 1000\,\mathrm{W/m^2K}$ ($Bi = 0.1$). The flat film thickness h_N is varied between 54 and 116 μm, corresponding to $0.5 < Re < 5$. Finally, to evaluate the three-dimensionality of the developed wave patterns, we use the energies of deformation in each direction, noted $E_x(t)$ and $E_z(t)$, as defined in [10]; given a computational domain of size $L_x \times L_z$, discretized with $M \times N$ regularly spaced grid points with coordinates $x_i = iL_x/M$ and $z_j = jL_z/N$, they have the forms

$$E_x(t) \equiv \frac{1}{MN}\sum_{j=0}^{N-1}\left(\sum_{m=1}^{M/2-1}|a_m(z_j,t)|^2\right)^{1/2},$$

$$E_z(t) \equiv \frac{1}{MN}\sum_{i=0}^{M-1}\left(\sum_{n=1}^{N/2-1}|b_n(x_i,t)|^2\right)^{1/2},$$

where the spatial Fourier coefficients are defined by

$$a_m(z,t) = \sum_{i=0}^{M-1} h(x_i,z,t)\,e^{\mathrm{i}\,2\pi m i/M},$$

$$b_n(x,t) = \sum_{j=0}^{N-1} h(x,z_j,t)\,e^{\mathrm{i}\,2\pi n j/N},$$

and $i = \sqrt{-1}$ is the imaginary unit. As an example, $E_x \ll E_z$ indicates that the deformation occurs mainly in the transverse direction with practically no deformation in the streamwise direction (though we can still have flow in the streamwise direction).

Figure 1 depicts snapshots of the free-surface evolution for a small Reynolds number and reveals the process by

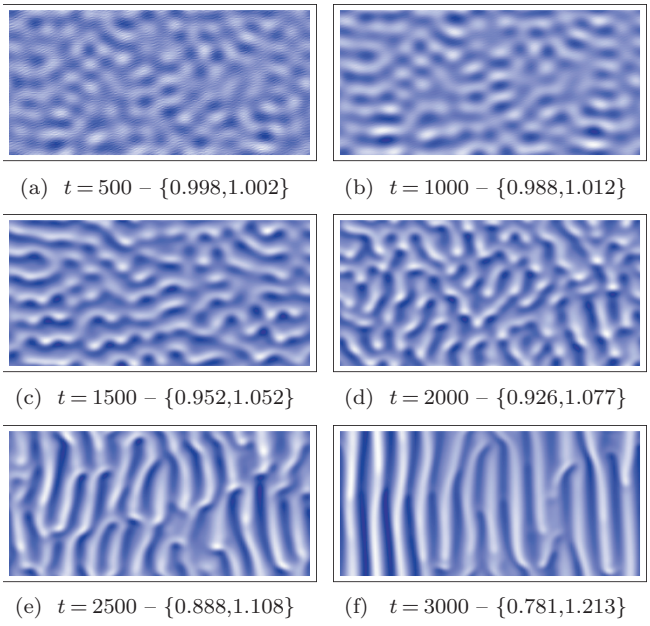

(a) $t = 500$ – {0.998,1.002} (b) $t = 1000$ – {0.988,1.012}

(c) $t = 1500$ – {0.952,1.052} (d) $t = 2000$ – {0.926,1.077}

(e) $t = 2500$ – {0.888,1.108} (f) $t = 3000$ – {0.781,1.213}

Fig. 1: (Colour on-line) Water film free surface at different times for $Re = 0.5$. Bright (dark) zones correspond to elevations (depressions) of the film whose extrema are given in brackets.

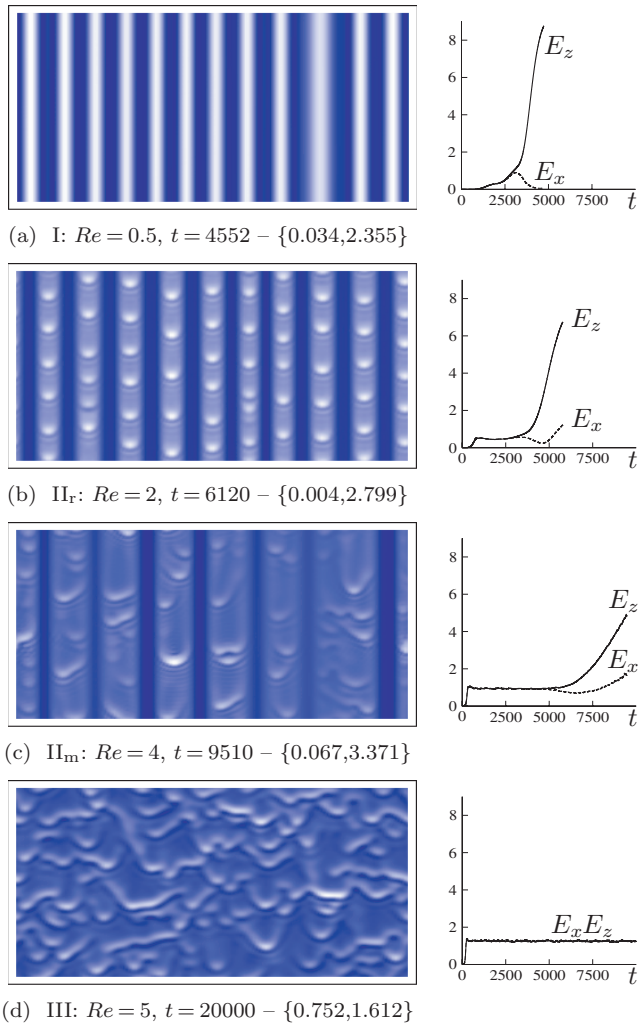

(a) I: $Re = 0.5$, $t = 4552$ – {0.034,2.355}

(b) $\mathrm{II_r}$: $Re = 2$, $t = 6120$ – {0.004,2.799}

(c) $\mathrm{II_m}$: $Re = 4$, $t = 9510$ – {0.067,3.371}

(d) III: $Re = 5$, $t = 20000$ – {0.752,1.612}

Fig. 2: (Colour on-line) Typical wave pattern for each regime (or phase). See legend of fig. 1. The times for (a-c) are near rupture. Plots show streamwise (E_x) and transverse (E_z) energies of deformations.

which rivulets are formed due to the Marangoni effect: the formation of circular patterns at early stages (a) reminiscent of the onset of (thermal) dewetting patterns on horizontal substrates [19–21] (due to the small flow rate) is followed by the development of a 2D periodic wave train (b,c) together with drop-like accumulation that breaks the 2D waves into 3D patterns (d), forming meanders (e,f) and finally rivulet structures aligned with the flow whose snapshot right before rupture is shown in fig. 2a. By increasing the Reynolds number, distinct wave regimes can be observed as shown in fig. 2. Furthermore, the evolution of energy of deformations enables to rationalize their qualitative differences just before rupture: I) $E_x \searrow$, $E_z \nearrow$ —hydrodynamic waves are damped in time while regularly spaced rivulets grow until rupture; II) $E_x \nearrow$, $E_z \nearrow$ —quasi-2D pulses ride the crests of rivulets; III) $E_x \approx E_z \sim$ const —fully 3D waves develop with no rupture. In regime III the two energies are very close to each other as the transverse modulations are now due to hydrodynamics. Regime II corresponds to spontaneous channeling of quasi-2D solitary pulses, which are either regular ($\mathrm{II_r}$) or transversely modulated ($\mathrm{II_m}$). Physical mechanisms dominating each regime are detailed below.

Regime I is purely dominated by thermocapillary effects, and is the only one that can be described by the single-film equation MBE [10,19]. Indeed, as Re increases, the amount of fluid in the rivulets increases, which then increases the local film thickness, hence the "local Reynolds number", which is in favor of the hydrodynamic instability triggered by inertia. But at the same time the rivulets have a stabilizing effect on the pulses: as the width of a rivulet is constant in the streamwise direction (whether a pulse is present or not), the transverse curvature $\partial_{zz}h$ increases with the local thickness h (*i.e.* when a pulse is present). As a result the induced capillary pressure is larger in the hump of the pulses than in the flat zones in-between which then creates a pressure gradient that drags some liquid out of the humps thus reducing their amplitudes. The competition between the two above mechanisms (inertia and streamwise capillarity) is responsible for the transition I-$\mathrm{II_r}$. In $\mathrm{II_m}$ the quasi-2D solitary pulses riding the rivulets experience a transverse instability, which, however, does not lead to their complete disintegration. An analogy can be made here with isothermal films on a vertical planar substrate where isolated 2D solitary waves experience an instability in the transverse direction leading to 3D wave patterns [18]. As Re then increases from $\mathrm{II_r}$ (fig. 2b) to $\mathrm{II_m}$ (fig. 2c), the mean radius of curvature of the rivulets

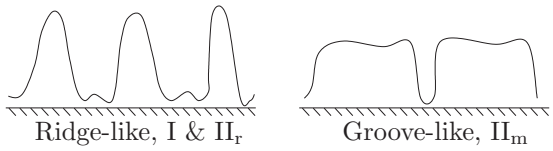

Fig. 3: Cross-section of rivulet structures induced by lateral thermocapillary flow. A *ridge-like structure* has quasi-two-dimensional solitary waves riding on them while a *groove-like structure* allows for transverse modulations of solitary pulses.

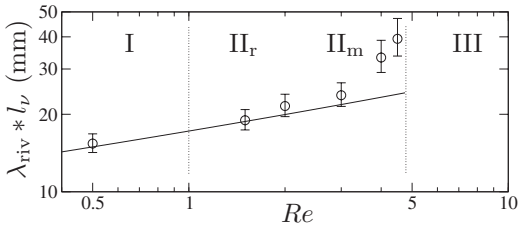

Fig. 4: Wavelength of the rivulets obtained by simulation of our model (circles) and from linear stability analysis (solid line). Dotted lines separate the different phases.

increases thus approaching the "planar" limit and the waves riding the rivulets are more prone to transverse instabilities. Topological differences are sketched in fig. 3. In II_r (like in I) rivulets form "ridges" while in II_m the situation looks more like "grooves" that split the film into channels wide enough for the 3D hydrodynamic waves to survive; 7 grooves in fig. 2c. Finally, regime III is dominated by inertia effects with little or no influence of thermocapillarity. The transition II-III thus occurs at some Re when the film does not rupture.

Wavelengths of rivulet structures are reported in fig. 4 (circles) along with the different phases described in fig. 2. The solid line shows the linear stability result found from the pure thermocapillary problem [9] or equivalently from our model by suppressing the streamwise dependence: $\lambda_{riv} = 4\pi(1 + Bi\bar{h}_N)(\Gamma\bar{h}_N/3BiMa)^{1/2}$ with $\bar{h}_N \equiv h_N/l_\nu = \sqrt[3]{3Re}$ the dimensionless flat film thickness. Importantly, notice that the transition II_r-II_m coincides with the departure of the wavelength from its linear prediction, signature of transversely modulated solitary-wave dynamics along the rivulets.

To conclude, we have found regimes of spontaneous channeling of quasi-2D solitary pulses and have determined their conditions of existence. These regimes should be particularly attractive from the experimental point of view, especially as fluid flow settings where 2D waves can be stabilized are quite rare. The novelty of the resulting pattern might very well be generic for systems exhibiting a competition between monotonic and oscillatory (or wave) instabilities with anisotropy (here, due to the direction of the basic flow).

* * *

We are grateful to P. Manneville for fruitful discussions and to J.-C. Dupin for help with the figures. BS, PC and SK gratefully acknowledge financial support from, respectivly, BELSPO (Belgian Science Policy) and ESA (European Space Agency), from the Fonds de la Recherche Scientifique - FNRS, and from EPSRC (Engineering and Physical Sciences Research Council).

REFERENCES

[1] Manneville P., *Dissipative Structures and Weak Turbulence* (Academic Press, New York) 1990.
[2] Saprykin S., Demekhin E. A. and Kalliadasis S., *Phys. Rev. Lett.*, **94** (2005) 224101.
[3] Alekseenko S. V., Nakoryakov V. E. and Pokusaev B. G., *Wave Flow in Liquid Films*, 3rd edition (Begell House, New York) 1994.
[4] Liu J., Schneider J. B. and Gollub J. P., *Phys. Fluids*, **7** (1995) 55.
[5] Park C. D. and Nosoko T., *AIChE J.*, **49** (2003) 2715.
[6] Smith K. A., *J. Fluid Mech.*, **24** (1966) 401.
[7] Oron A., Davis S. H. and Bankoff S. G., *Rev. Mod. Phys.*, **69** (1997) 931.
[8] Colinet P., Legros J. C. and Velarde M. G., *Nonlinear Dynamics of Surface-Tension-Driven Instabilities* (Wiley-VCH, New York) 2001.
[9] Goussis D. A. and Kelly R. E., *J. Fluid Mech.*, **223** (1991) 25.
[10] Joo S. W., Davis S. H. and Bankoff S. G., *J. Fluid Mech.*, **321** (1996) 279.
[11] Yih C.-S., *Phys. Fluids*, **6** (1963) 321.
[12] Lin S. P., *J. Fluid Mech.*, **63** (1974) 417.
[13] Scheid B., Ruyer-Quil C., Thiele U., Kabov O. A., Legros J. C. and Colinet P., *J. Fluid Mech.*, **527** (2005) 303.
[14] Ramaswamy B., Krishnamoorthy S. and Joo S. W., *J. Comput. Phys.*, **131** (1997) 70.
[15] Ooshida T., *Phys. Fluids*, **11** (1999) 3247.
[16] Ruyer-Quil C. and Manneville P., *Eur. Phys. J. B*, **15** (2000) 357.
[17] Ruyer-Quil C., Scheid B., Kalliadasis S., Velarde M. G. and Zeytounian R. Kh., *J. Fluid Mech.*, **538** (2005) 199.
[18] Scheid B., Ruyer-Quil C. and Manneville P., *J. Fluid Mech.*, **562** (2006) 183.
[19] Bestehorn M., Pototsky A. and Thiele U., *Eur. Phys. J. B*, **33** (2003) 457.
[20] VanHook S. J., Schatz M. F., Swift J. B., McCormick W. D. and Swinney H. L., *J. Fluid Mech.*, **345** (1997) 45.
[21] Oron A., *Phys. Fluids*, **12** (2000) 1633.